

MICROSTRUCTURAL INVESTIGATIONS OF THE SHOT PEENED STEEL 42 CrMo 4 IN DIFFERENT HEAT TREATMENT CONDITIONS BY THE AID OF A X-RAY PROFILE ANALYSIS

F. Burgahn, O. Vöhringer and E. Macherauch,
Institut für Werkstoffkunde I, Universität Karlsruhe, D-7500 Karlsruhe, FRG

ABSTRACT

The dislocation density in the surface layers of shot peened materials changes in a characteristic way with the distance from surface and the hardness of the material. The determination of the dislocation density ρ_t , especially at high ρ_t -values, with the transmission electron microscopy is very difficult. However, the X-ray interference profile analysis allows this determination in an integral manner. Therefore, it is necessary to separate from a real profile the physical profile f using a standard specimen of the instrumental broadened profile h . The profiles are approximated with the Voigt-function, a convolution of Gauss- and Cauchy-functions. Then, the physical profile f is set to calculate the mean microstrain $\langle \epsilon^2 \rangle^{1/2}$ and the domain size D . In special circumstances, it is possible to estimate the dislocation density ρ_t , because $\rho_t = \langle \epsilon^2 \rangle^{1/2} D$.

Results of a single line analysis will be presented for the shot peened steel 42 CrMo 4 (AISI 4140) in different heat treatment conditions. The microhardness, the macro residual stresses, the mean microstrain and the domain sizes versus distance from surface were evaluated. Shot peening causes an increase in the mean microstrain near the surface (workhardening) for materials with a microhardness lower than 400 HV0.3 in the unpeened condition. Materials with a microhardness larger than 500 HV0.3 worksoften as a result of shot peening induced changes in the microstructure. Shot peening causes a decrease of the domain size in material states with low hardness. At high hardness, the domain size will be not influenced. These findings will be discussed together with shot peening induced changes in the microstructure.

KEYWORDS

Residual stress, half width, dislocation density, microstrain, domain size, profile analysis, workhardening, worksoftening.

INTRODUCTION

Extensive investigations were made to analyse the microstructural changes in the surface regions of shot peened metallic materials. Shot peening induced plastic deformation produces considerable changes of dislocation density and dislocation structure in the surface layers. Rearrangement, multiplication and annihilation of dislocations are the microstructural consequences of shot peening [1]. Therefore, the quantitative description of the microstructure of shot peened surface regions is necessary for the estimation of the mechanical behaviour of shot peened components. However, it is very difficult to carry out quantitative investigations of the microstructure at large dislocation densities using transmission electron microscopy. In this case, the X-ray interference line profile analysis allows a microstructural characterization in an integral manner. The shape of interference line profile is used to calculate the domain size (coherent scattering regions) and the mean strain $\langle \epsilon^2 \rangle^{1/2}$. In special cases, the ratio $\langle \epsilon^2 \rangle^{1/2}/D$ is proportional to the dislocation density ρ_{\perp} . Besides the difficult multiple line analysis [2,3], the single line analysis [4-7] allows the quick calculation of the microstructural data. The physical true profile f is determined with the typical parameters of the broadened profile h and the standard profile g . These parameters are calculated after approximation of the profiles with a Voigt-function, which is the convolution of Cauchy- and Gauss-functions.

EXPERIMENTAL DETAILS

The experiments were carried out using a plate of 42 CrMo 4 (AISI 4140) with the dimensions $500 \times 20 \times 1000 \text{ mm}^3$. The chemical composition of this steel in wt.-% was 0.44 C, 0.22 Si, 0.59 Mn, 1.05 Cr, 0.21 Mo, 0.04 Cu, 0.06 Ni, 0.01 P, 0.01 S and the rest Fe. Workpiece sheets with the dimensions $110 \times 20 \times 2.2 \text{ mm}^3$ were manufactured. The normalized state was produced by annealing 3 h at $930 \text{ }^{\circ}\text{C}$ in vacuum and subsequent slow furnace cooling. Other specimens were annealed 20 min at $850 \text{ }^{\circ}\text{C}$ in a fluidized bed furnace with nitrogen as circulation gas and were then quenched in oil. The following tempering in vacuum for 2 h at the temperatures $450 \text{ }^{\circ}\text{C}$ and $650 \text{ }^{\circ}\text{C}$ resulted in characteristic quenched and tempered material states. After all these heat treatments, all specimens were ground to their final thickness of 2 mm for the purpose of removing surface oxidation and decarbonization.

The shot peening treatments were carried out with an air blast machine using a cast steel shot S 330 (hardness of 55 to 58 HRC) with a pressure of 3 bar, a coverage of $3 \times 98 \%$ and an Almen intensity of 0.21 mmC.

The macro residual stresses were determined by X-ray measurements using a ψ -diffractometer and applying the $\sin^2\psi$ -method [8]. For this purpose, the shifting of the {211}-interference lines with $\text{CrK}\alpha$ -radiation was measured. The stress measurements of subsurface layers were carried out after removing the surface layers of both sides of the specimen with the aid of a chemical polishing technique. After removing the surface layers, the residual stress distributions as a function of the distance from surface were corrected with the method according to [9]. The microhardness HV0.3 was estimated after every polishing procedure. The X-ray single line analysis was carried out at the {110}-interference line which was measured with $\text{CoK}\alpha$ -radiation in the interval of 48.5° to 56.5° with a stepsize of $0.02^{\circ} 2\theta$.

In order to determine the domain size D and the mean strain $\langle \epsilon^2 \rangle^{1/2}$, the Voigt-single line analysis [4-7] was used which calculates the Cauchy- and the Gauss-parts of the physical true interference line profile f . The standard profile g was determined using a well annealed 42 CrMo 4. After subtraction of the background, all profiles were corrected with the Lorentz- and polarization-factor and α_2 -removal, using the method of [10].

RESULTS

Fig. 1a shows the macro residual stress state after shot peening as a function of the distance from surface. In the normalized material state, the maximum of the compressive residual stresses lies on the direct surface.

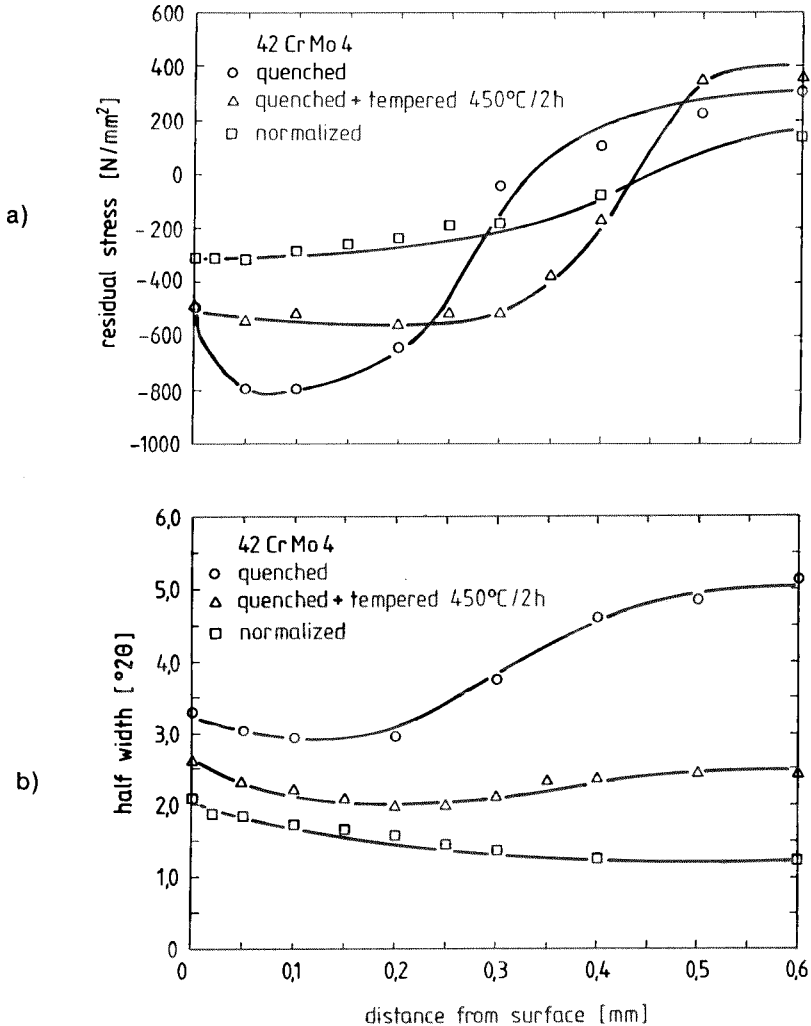


Fig. 1 Residual stress (a) and half width of X-ray interference lines (b) vs. distance from surface of shot peened 42 CrMo 4 in different heat treatment conditions

With increasing distance from surface the amounts of the residual stresses decrease until they reach zero at the depth $x = 0.45$ mm where the sign of the macro residual stresses changes. In quenched and tempered (450°C/2h) and water quenched material states, the compressive residual stresses maxima lie below the surface. These maxima increase with increasing hardness. The penetration depth of shot peening induced compressive residual stresses, however, decreases. Fig. 1b shows for all material states the half width breadths at half maximum of the $\{211\}$ -interference profile line as a function of distance from surface. In the normalized state, the half width breadth decreases with increasing

depth. In the quenched and tempered and in the water quenched material state, the half width breadths decrease and obtain minimum values with increasing depth (in water quenched at a smaller distance from surface than in quenched and tempered material state). Then, an increase up to constant plateau values at a depth larger than 0.5 mm is observed. In quenched and tempered material states, this plateau value is smaller than the half width breadth at the surface. The plateau value of the water quenched material state, however, is 60 % larger than the half width breadth at the surface. These results agree with many other investigations concerning the characterization of shot peened surface layers [1].

Fig. 2 shows the values of the microhardness HV0.3 for all material states as a function of distance from surface. With the exception of the quenched and tempered material

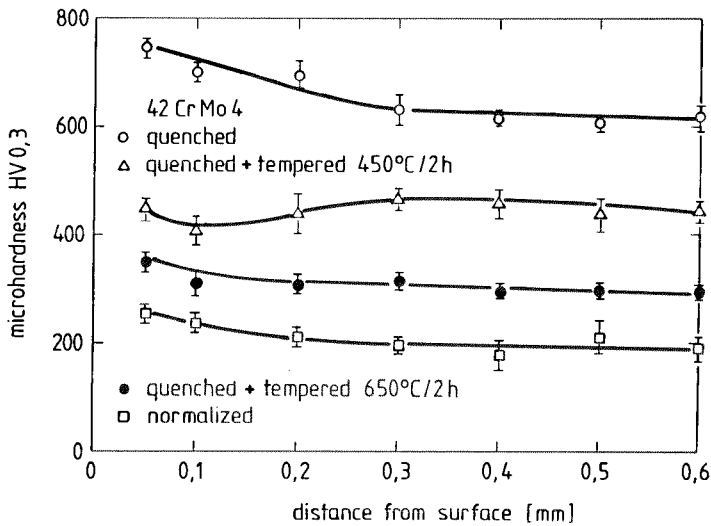


Fig. 2 Microhardness HV0.3 vs. distance from surface of shot peened 42 CrMo 4 in different heat treatment conditions

state (450°C/2h), the microhardness decreases with increasing distance from surface and, at a depth of 0.3 mm, reaches a plateau value resulting from the heat treatment.

The mean strain values calculated with the aid of the single line profile analysis using the {110}-interference lines are shown in Fig. 3 as a function of distance from surface. The normalized and the quenched and tempered (650°C/2h) material state are characterized by mean strain values $\langle \epsilon \rangle^{1/2}$ which decrease with increasing depth. This behaviour corresponds to that of the half width breadth of the normalized material state (Fig. 1b). In the quenched and tempered (450°C/2h) material state, the mean strain values at first decrease and then, after reaching a minimum at a depth of $x = 0.2$ mm, the $\langle \epsilon^2 \rangle^{1/2}$ -values increase with increasing distance from surface.

In contrast to this, in the quenched state, there are hardly any changes of the mean strain values down to a depth 0.2 mm. Below 0.2 mm, however, the mean strain values rapidly increase. For the two last-mentioned material states, the development of the $\langle \epsilon^2 \rangle^{1/2}$ -values is similar to that of the half width values (Fig. 1b). On the whole, the $\langle \epsilon^2 \rangle^{1/2}$ -values rapidly increase with increasing hardness.

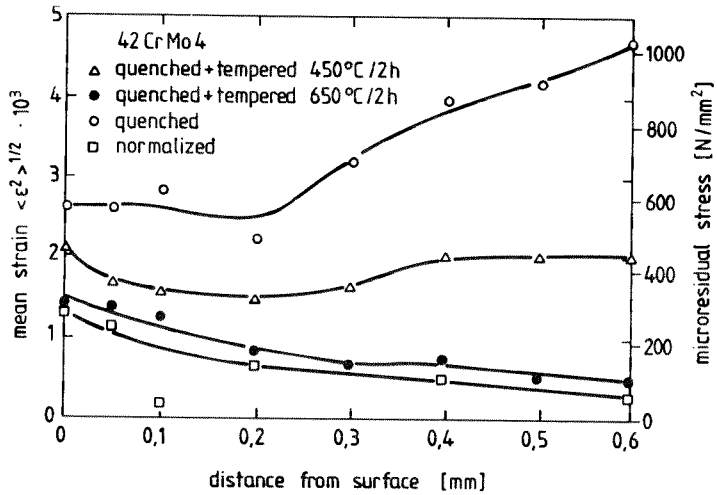


Fig. 3 Mean strain $\langle \epsilon^2 \rangle^{1/2}$ vs. distance from surface of shot peened 42 CrMo 4 in different heat treatment conditions

The size of coherent scattering regions, the domain size D , is shown in Fig. 4 as a function of distance from surface. Shot peening of the water quenched material state induces no changes with regard to the distance from surface. With decreasing hardness, the D -values increase and reach plateau values in regions below a depth of 0.5 mm, which are not influenced by shot peening. It can fundamentally be stated that the D -values decrease with increasing hardness.

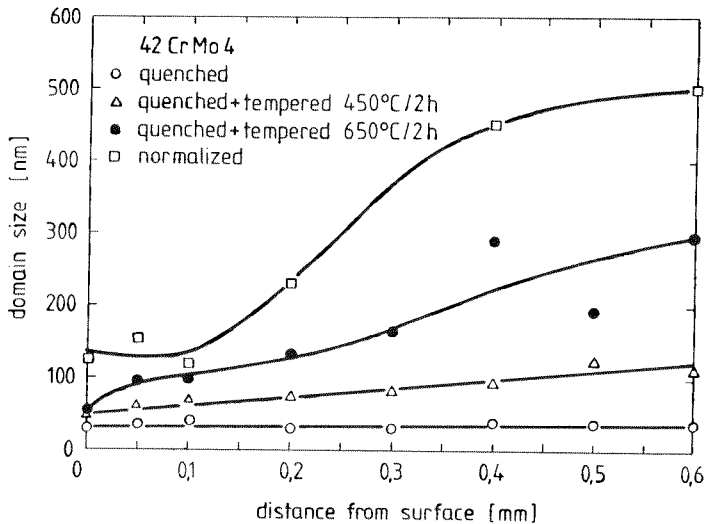


Fig. 4 Domain size D vs. distance from surface of shot peened 42 CrMo 4 in different heat treatment conditions

DISCUSSION

The half width value of X-ray interference lines [see e. g. 1], which is often used to characterize the workhardening state of the shot peened surface, shows - as can be seen from a comparison between the results of Fig. 1b and Fig. 3 - a dependence from the distance from surface which is qualitatively similar to that of the mean strain $\langle \varepsilon^2 \rangle^{1/2}$. A quantitative characterization and estimation of these results is, however, only possible if the $\langle \varepsilon^2 \rangle^{1/2}$ -values and the determined domain sizes are known.

However, some difficulties arise concerning the physical interpretation of these parameters. Nevertheless, different parameter studies revealed that D can be correlated with the mean distance between dislocations and hence with the dislocation density and with the mean diameter of dislocation cells [see e. g. 11]. Thus, the domain size of steels having been differently heated treated only depends on the dislocation density and the dislocation arrangement. The mean strains of the coherent scattering regions, however, are determined by the residual stress fields of the dislocations and by carbon atoms which may still exist in solid solution. Hence, the mean undirected micro-residual stresses are calculated according to [12,13] with equation

$$\sigma_{\text{micro}}^{\text{rs}} = E_{\langle hkl \rangle} \cdot \langle \varepsilon^2 \rangle^{1/2} \quad (1)$$

$E_{\langle hkl \rangle}$ is Young's modulus which acts perpendicularly to the X-ray measured lattice plane {hkl}. If the broadening of the X-ray interference profile line is only induced by dislocations, the dislocation density can be estimated according to eq. 2 [14,15] from the ratio of the mean strains and the domain size (b being the amount of the Burgers vector):

$$\rho_{\text{t}} = \frac{2\sqrt{3}}{b} \cdot \frac{\langle \varepsilon^2 \rangle^{1/2}}{D} \quad (2)$$

At mean dislocation densities, a good agreement exists between the ρ_{t} -values determined by the X-ray profile analysis and those obtained with the transmission electron microscopy [16,17]. At high dislocation densities ($\rho_{\text{t}} > 10^{10} \text{ cm}^{-2}$), the TEM-method fails, whereas the X-ray line profile analysis allows the integral determination of ρ_{t} -values provided that the mean strain effect of possibly existing soluted foreign atoms is negligible.

The right-hand part of Fig. 3 shows the micro residual stresses calculated according to eq. (1) from the mean strains with $E_{\langle 110 \rangle} = 220\,000 \text{ N/mm}^2$. Hence, in normalized material states, shot peening causes an increase of $\sigma_{\text{micro}}^{\text{rs}}$ of about 60 N/mm^2 in the regions which are not influenced by shot peening (distance from surface $\geq 0.5 \text{ mm}$) to about 290 N/mm^2 directly at the surface. This increase of micro residual stresses is only caused by dislocation hardening processes, as will be explained below. In the water quenched material state, however, a worksoftening effect occurs, which leads to a decrease of the micro residual stresses from approximately 1030 N/mm^2 - in the regions which are not influenced by shot peening ($x \geq 0.5 \text{ mm}$) - to 580 N/mm^2 directly at the surface layer. The micro residual stress values of the quenched and tempered states lie between the above-mentioned values, depending on the hardness of the material.

A measure of the workhardening and worksoftening behaviour of a material is given by the ratio $\langle \varepsilon^2 \rangle^{1/2}/D$, the so-called "dislocation density parameter", which is according to eq. (2) proportional to the dislocation density. This ratio is shown in Fig. 5 as a function of the distance from surface. In the case of the normalized and the two quenched and tempered material states, this ratio increases with decreasing distance from surface. This effect is the more pronounced the lower the hardness of these material conditions is. These changes are mainly the result of shot peening induced hardening effects due to dislocation multiplication. As shown in Fig. 6, the dislocation density, in this case for the unpeened condition, increases by a factor of 18 in the normalized state and by a factor

of 16 and 2.5 in quenched and tempered material states.

In the water quenched condition, the observed decrease of the relatively large ratio $\langle \epsilon^2 \rangle^{1/2} / D$ to smaller distances from surface (Fig. 5) is caused by dislocation rearrangements with high initial density, by dislocation annihilations and by dislocation slip induced rearrangements of soluted carbon atoms into positions with lower distortion [1].

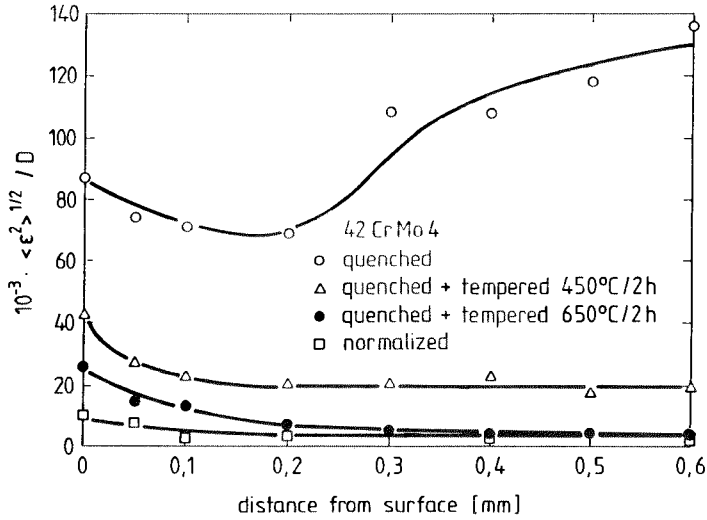


Fig. 5 Dislocation density parameter $\langle \epsilon^2 \rangle^{1/2} / D$ vs. distance from surface

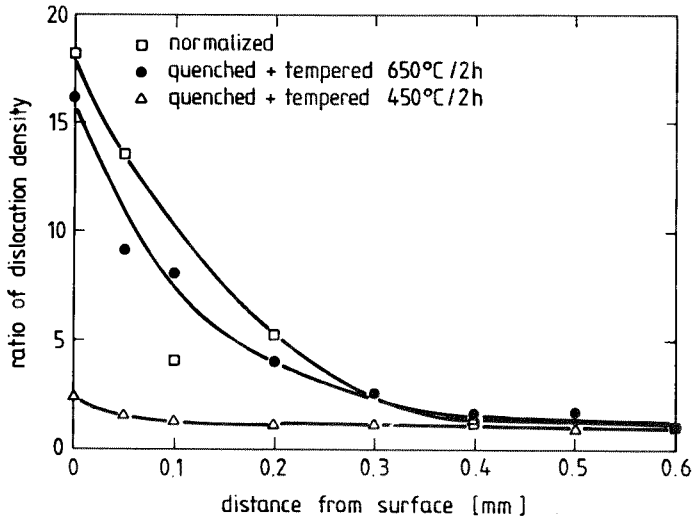


Fig. 6 Ratio of dislocation density vs. distance from surface

The shot peening induced workhardening and worksoftening processes are assessed from the point of view of the material state as shown in Figs. 7a and b where the mean

strain or mean micro-residual stress and the domain size are drawn versus the microhardness of the unpeened material state.

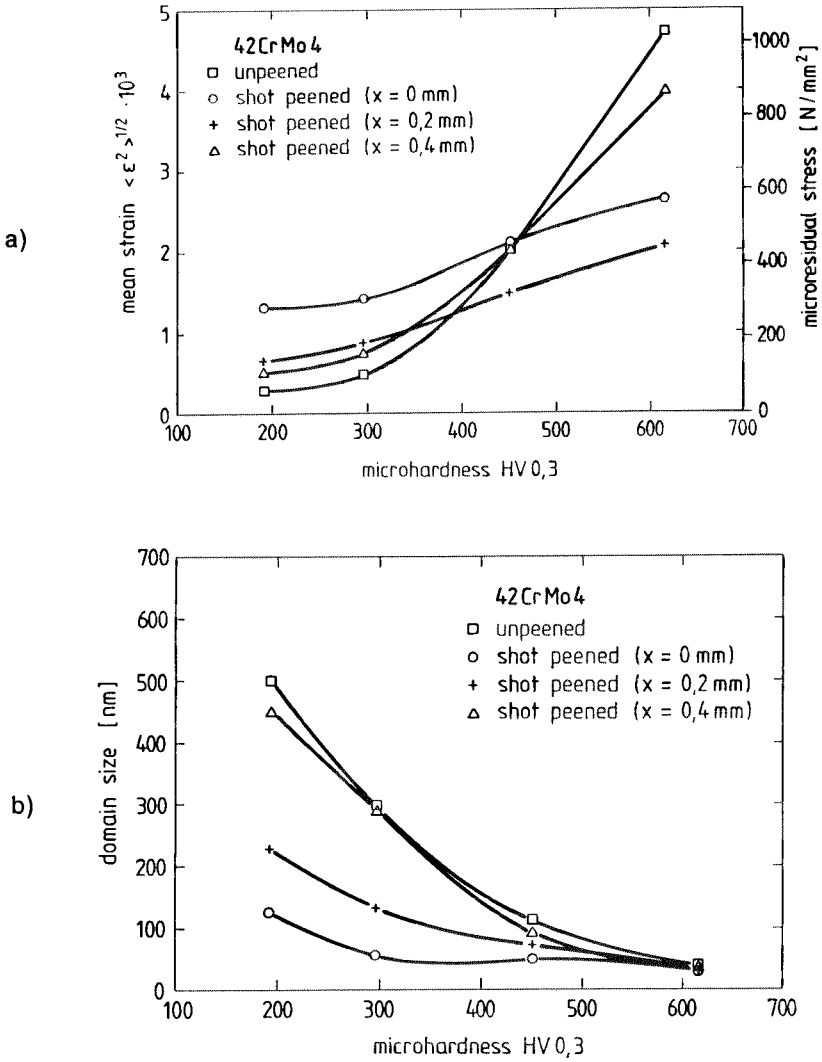


Fig. 7 Mean strain $\langle \epsilon^2 \rangle^{1/2}$ (a) and domain size D (b) of unpeened and shot peened material states (x = distance from surface) as a function of microhardness HV0.3 in the unpeened condition

The comparison of $\langle \epsilon^2 \rangle^{1/2}$ or σ_{micro} of unpeened and shot peened surface conditions ($x = 0$ mm) reveals that shot peening induces microstructural workhardening (hardness HV0.3 ≤ 460) or worksoftening (hardness HV0.3 ≥ 460). These findings agree with results obtained on different quenched and tempered steels [16]. The workhardening and worksoftening processes occur also below the surface layer, even if the shot peening influence becomes weaker with increasing distance x , as is shown by the curves for

$x = 0.2$ and 0.4 mm. With increasing hardness, the domain size decrease (Fig. 7b) as a result of increasing dislocation density or decreasing dislocation distances. The reduction of domain size is the less the more pronounced the peening induced local deformations in the examined layer are.

Finally, an obvious disagreement shall be discussed which is found when comparing the micro residual stress and the microhardness vs. distance from surface of different shot peened material states (Fig. 2 and 3). In the normalized condition, shot peening induced workhardening is described by similar dependencies of the microhardness and the micro residual stress vs. distance from surface. However, in the water quenched condition, shot peening induces a decrease of the microresidual stress and an increase of the microhardness. This finding was already discussed in [1] and explained by additional hardness resistance and smaller indentation, respectively, which are a result of a hydrostatic compressive residual stress state. Therefore, it can finally be stated that for the characterization of a shot peened surface state, especially of quenched and tempered workpieces, the parameters of the X-ray line profile analysis are better suited than the results of microhardness measurements which are always connected with local changes in the material state.

REFERENCES

- [1] Vöhringer, O.: In Proc. 3rd Int. Conf. Shot Peening, DGM-Informationsgesellschaft, Oberursel (1987), 185/204
- [2] Warren, B.E.: Progress in Metal Physics 8 (1959), 147/202
- [3] Warren, B.E.; Averbach, B.L.: Journ. Appl. Phys. 21 (1950), 595/599
- [4] Delhez, R.; De Keijser, Th.H.; Mittemeijer, E.J.: Surface Engineering 3 (1987), 331/342
- [5] De Keijser, Th.H.; Langford, J.I.; Mittemeijer, E.J.; Vogels, A.B.P.: Journ. Appl. Cryst. 15 (1982), 308/314
- [6] Langford, J.I.: Journ. Appl. Cryst. 11 (1978), 10/14
- [7] Schöning, F.R.L.: Acta Cryst. 18 (1965), 975/976
- [8] Macherauch, E.; Müller, P.: Z. Angew. Physik 13 (1961), 305/312
- [9] Moore, M.G.; Evans, W.P.: SAE Trans. 66 (1958), 340/345
- [10] Delhez, R.; Th.H.; Mittemeijer, E.J.: J. Appl. Cryst. 8 (1975), 609/611
- [11] Faber, H.; Vöhringer, O.; Macherauch, E.: Härterei-Tech. Mitt. 34 (1979), 1/9
- [12] Wolfstieg, U.: Dissertation Universität Köln (1955)
- [13] Wolfstieg, U.; Macherauch, E.: Eigenspannungen, DGM-Informationsgesellschaft, Oberursel (1979), 345/354
- [14] Williamson, G.K.; Smallman, R.E.: Phil. Mag. 1 (1956), 34/46
- [15] Mikkola, D.E.; Cohen, J.B.: Metall. Soc. Conf., Vol. 36, Gordon and Breach Sci. Publ. (1965), 289/333
- [16] Evans, W.P.; Rickleffs, R.E.; Millian, J.F.: Metall. Soc. Conf., Vol. 36, Gordon and Breach Sci. Publ. (1965), 351/377
- [17] Burgahn, F.: Unpublished results, University of Karlsruhe (1990)